Evolution of opsin genes in closely-related species of butterflies specialized in different microhabitats

Joséphine Ledamoisel, Andrew Dang, Julien Devilliers, Tiphaine Marvillet, Sophie Lemoine, Manuela Lopez-Villavicencio, Adriana Briscoe, Vincent Debat, Violaine Llaurens

Evolution of opsin genes in closely-related species of butterflies specialized in different microhabitats

Joséphine Ledamoisel[1,2], Andrew Dang[3], Julien Devilliers[2], Tiphaine Marvillet[4], Sophie Lemoine[4], Manuela Lopez-Villavicencio[2], Adriana Briscoe[3], Vincent Debat[2], Violaine Llaurens[1]

1. Centre Interdisciplinaire de Recherche en Biologie (UMR 7241, Collège de France/CNRS/INSERM), Paris, France.
2. Institut de Systématique, Evolution et Biodiversité (ISYEB UMR 7205), Muséum National d'Histoire Naturelle, Paris, France.
3. Department of Ecology and Evolutionary Biology, UC Irvine, Irvine, CA, USA.
4. GenomiqueENS, Institut de Biologie de l'ENS (IBENS), Département de biologie, École normale supérieure, CNRS, INSERM, Université PSL, 75005 Paris, France

*Corresponding author

Email: josephine.ledamoisel@outlook.fr (JL)

Abstract

Multiple selective pressures can shape the evolution of color vision in animals, by acting on the co-evolution of the opsin genes. How do adaptive processes shape the duplications of opsins, the evolution of their amino acids and the modification of their patterns of expression? At large phylogenetic scales, natural selection due to the contrasted light environments has been found to have a profound impact on the evolution of the opsin gene family. However, in closely-related species, species interactions due to sexual selection or competition may also influence opsin evolution. Here, we investigate the diversification of opsin sequences and their expression in closely-related blue *Morpho* butterfly species, living in different microhabitats, to shed light on the effect of biotic and abiotic selective pressures shaping the evolution of their opsin gene family. First, we combined genomics, transcriptomics and immunochemistry to precisely characterize the expression and the spatial distribution of the opsin proteins found in the eyes of *Morpho helenor*. We found unique ommatidial types compared to other butterfly species. We then investigated the evolution of opsin genes among 18 *Morpho* species, found signature of positive selection on two opsin genes, and identified key co-evolving amino-acids shaping the diversification of the *Morpho* visual system. We showed that such opsin evolution was correlated to both light environment and wing coloration, highlighting the joint effect of several selective pressures in the evolution of those proteins. Overall, our study underlines the peculiar evolution of visual systems in closely-related species specialized in divergent microhabitats.

Introduction

The sensitivity to different wavelengths of light has been extensively studied in multiple species, and these studies have revealed striking diversification of color discrimination capacities throughout animals. Yet, the selective pressures generated by the light environment and the ecological interactions within and among species shaping the diversification of the opsin gene family are largely unknown in most animal species.

Opsin proteins have been shown to be much more diversified in the eyes of diurnal species compared to nocturnal species in both vertebrates (Musilova et al. 2021) and invertebrates (Sondhi et al. 2021), suggesting a prominent impact of selective pressures brought from the light environment on their evolution. Evidence of concerted evolution, due to gene duplication, mutations and gene conversion has been reported in the opsin gene family (Brandon et al. 2017). Variations in the amino-acid sequences of opsins can also directly influence the sensitivity of the opsin-chromophore complex known as a visual pigment to different light wavelengths, and the combination of opsins expressed within and among the different photoreceptor cells within the eye strongly impacts color discrimination (Hofmann and Lamb 2023). In insects, the chromophore bound to the opsin protein is 11-cis-hydroxy retinal (Smith and Goldsmith 1990) and the evolution of the light-absorbing properties of each visual pigment is strongly linked to the nature of amino acids located around this chromophore (Hofmann and Lamb 2023).

In Lepidoptera, phylogenetic reconstructions inferred an ancestral visual system with three main opsin proteins (Briscoe 2008): ultraviolet-sensitive opsins (*UVRh*), blue-sensitive opsins (*BRh*), and long wavelength-sensitive opsins (*LWRh*). However, in many butterfly families, multiple events of opsin gene duplications and mutations affecting the chromophore-interacting amino-acids have been documented (Arikawa 2003; Chen et al. 2016). The duplication of opsin genes, accompanied by shifts in their spectral sensitivity, has been shown to result in the absorbance of a wider wavelength range, as for instance in Nymphalidae (Frentiu et al. 2007) or Lycaenidae (Sison-Mangus et al. 2008). Variation in the combination of opsins with different amino-acid compositions in the binding pocket surrounding

the chromophore, as well as their distribution in different photoreceptive cells, shape the evolution of color discrimination capacities in butterflies (Stavenga and Arikawa 2006).

The compound eyes of butterflies are composed of ommatidia, formed by a cluster of nine photoreceptive cells (named R1 to R9), which may contain different sets of opsin proteins. Variations in the spatial expression of the different opsins within the different cell types, as well as in the spatial distribution of ommatidial types throughout the compound eyes also strongly influence the evolution of sensitivity to light and color discrimination (Arikawa 2003). The co-expression of opsins in cells has been documented in *Heliconius* butterflies, with *LWRh* and *BRh* co-expression participating in spectral-tuning (McCulloch et al. 2022). However, the discrimination of a wider range of colors is also influenced by the evolution of filtering pigments occurring within the ommatidia (Wakakuwa et al. 2004; Zaccardi et al. 2006). The evolution of color discrimination might therefore stem from various molecular and cellular processes: reconstructing the evolutionary steps leading to divergent visual systems thus requires investigating not only the evolution of opsins sequences, but also their levels of expression as well as their spatial distribution within and among ommatidia.

Identifying the respective contribution of the different selective pressures acting on the evolution of opsin properties and spatial distribution within the eyes is challenging, because vision is involved in multiple fitness-related traits in many animals, such as foraging (Zhang 2012), mate recognition (Smith et al. 2002; Gomez et al. 2010) and/or orientation (Franzke et al. 2020). Contrasted evolution of opsins has been shown among species living in different light environments (Horth 2007): for example, in aquatic environments, opsins were found to be differentially expressed between cichlids (Ricci et al. 2023) and cardinalfishes (Luehrmann et al. 2020) species living in different photic micro-habitats (shallow *vs*. deep waters). Ecological interactions can also shape the evolution of color discrimination capacities in animals. Visual cues are often used in mate choice and species recognition (in invertebrates; (Detto 2007), and in vertebrates; (Dollion et al. 2020), potentially promoting the selection of different

visual sensitivities in different taxa. As the display of bright colorations is often associated with traits contributing to fitness (*e.g.* boldness; (Godin and Dugatkin 1996), low parasite load; (Maan et al. 2006), body condition; (Pérez i de Lanuza et al. 2014)), sexual selection could favour the evolution of specific color sensitivity. The evolution of color discrimination could also be promoted between closely-related species sharing the same habitat, as poor species recognition could lead to substantial deleterious reproductive interference (Gröning and Hochkirch 2008), although the literature still lacks empirical evidence.

The rise of genomics has permitted the study of the evolution of opsin sequences at very large phylogenetic scales (Musilova et al. 2021; Murphy and Westerman 2022; Schott et al. 2024), highlighting an important effect of the light environment on the macro-evolution of visual systems. However, sexual selection is more likely to influence opsin evolution at a smaller phylogenetic scale, as revealed in fishes (Sandkam et al. 2015) and butterflies (Chakraborty et al. 2023). Investigating the diversification of opsin gene sequences and patterns of expression in closely-related species with contrasted ecologies can thus shed light on the respective effects of biotic and abiotic selective pressures shaping the evolution of the opsin gene family.

Here, we focus on the evolution of visual proteins within the neotropical butterfly genus *Morpho,* where sympatric species are distributed across different vertical forest strata (Chazot et al. 2016; Chazot et al. 2021), as well as different temporal niches (Le Roy et al. 2021). Such specialisation into different spatio-temporal microhabitats is associated with a strong heterogeneity in the light environment (Nilsson et al. 2022). The divergent light environment encountered by different *Morpho* species could thus influence the evolution of their color discrimination capacities. Furthermore, these different species strongly differ in the structural and pigmentary colors of their wings. Behavioral experiments carried out in blue *Morpho* species showed that iridescent blue coloration can be a cue used by males in intra or interspecific interactions, like male-male competition and female recognition (Le Roy et al. 2021; Ledamoisel et al. 2025). Consequently, as shades of iridescent blue vary between species, different sensitivities to blue

light could have evolved within this genus. In a lycaenid species displaying a blue wing color pattern, a blue opsin duplication was indeed detected (Sison-Mangus et al. 2006). Similarly, some *Heliconius* species displaying UV-colored pigments on their wings have accurate UV discrimination due to duplicated *UVRh* (Briscoe et al. 2010). Visual modelling combined with behavioral experiments revealed that this additional violet receptor could facilitate the discrimination of conspecifics during mate choice (McCulloch et al. 2017; Finkbeiner and Briscoe 2021), highlighting the effect of sexual interactions as selective agent acting on opsin evolution in butterflies.

The recent sequencing of the genomes of three blue *Morpho* species has revealed duplications in the *LWRh* opsins with three gene copies, in sharp contrast with other *Satyrinae* butterflies (Bastide et al. 2022), raising the question of the evolutionary origin of such duplications and of the selective regimes acting on the five opsin genes throughout the *Morpho* genus. Recent studies also investigated the different light sensitivities of the photoreceptor cells in the blue species *Morpho helenor* (Belušič et al. 2021; Pirih et al. 2022), also calling for an investigation of the spatial distribution of opsins in different photoreceptors.

We thus investigate the evolution of opsin gene sequences and expression in the genus *Morpho*, where divergent selection stemming from the light environment and from the wing coloration in closely-related species might have shaped the evolution of opsins properties. We conducted a comprehensive study of the visual system of *M. helenor* by characterizing all the sequences of opsin genes found in its genome, quantifying opsin mRNA expression in the eyes of males and females, and localizing the corresponding opsin proteins within the receptive cells in different ommatidia composing their retina. We then investigated the evolution of opsin genes among 18 *Morpho* species, by (1) testing for signature of selection against the null hypothesis of neutral evolution and (2) assessing the role of amino-acid co-evolution in shaping the diversification of their visual systems. In particular, we tested whether the ecological environment or the co-evolution with their wing coloration could have influenced the

diversification of their photosensitive proteins. Our study thus aims at identifying the ecological and molecular mechanisms driving the evolution of visual systems.

Results

Opsin diversity, expression and localization in the eye of M. helenor.

The complete coding sequences of the butterfly opsins were retrieved from the previously published *M. helenor* genome (Bastide et al. 2022) allowing recovery of the three *LWRh* genes (further referred as *LW1Rh*, *LW2Rh* and *LW3Rh*), as well as the *UVRh* and *BRh* genes. We established contig-to-chromosome correspondence between the *M. helenor* genome assembly and the *Maniola jurtina* reference chromosomes and found that *LW1Rh*, *LW2Rh* and *LW3Rh* genes were located collinearly on the contig corresponding to chromosome 4 in *M. jurtina*. In contrast, *UVRh* and *BRh* were found on the contig corresponding to chromosome 9, separated by a distance of approximately 4 to 6 Mb (see Table S1). An Illumina analysis of the eye RNA expression confirmed that all five opsin genes (*UVRh*, *BRh*, *LW1Rh*, *LW2Rh* and *LW3Rh*) are expressed in the eye tissues of both males and females. A differential gene expression analysis did not reveal any differential expression of those opsin genes between sexes (Figure S1). However, individual ANOVAs performed on the expression levels of each opsin gene separately show that females express more *LW1Rh* (Kruskal-Wallis test; *adjusted p-value* = 0.045) and *LW2Rh* (Kruskal-Wallis test; *adjusted p-value* = 0.045) opsin genes than males (Figure S2).

UVRh, BRh, *and* LW1Rh *opsin proteins are expressed in the R1 and R2 photoreceptor cells of* Morpho helenor *eyes.*

Using custom polyclonal antibodies, we then specifically characterized the localization of the *UVRh*, *BRh* and *LW1Rh* opsin proteins within *M. helenor* eyes using an immunochemistry approach. We found expression of the *UVRh*, *BRh*, and *LW1Rh* opsin proteins in the R1 and R2 photoreceptors of both female and male specimens of *M. helenor* (Figure 1 A & B). There was no cross reaction between these three antibodies and we saw no evidence of co-localization of *BRh*, *UVRh*, or *LW1Rh*.

The proportion of cells expressing the different opsin proteins was strongly uneven: while more than half of the photoreceptor cells expressed the *BRh* opsins in both males and females, the proportion of photoreceptor expressing *UVRh* and *LW1Rh* was around 20% each, in both sexes (Figure S3). Although the retina of both males and females expressed a majority of *BRh* photoreceptors, males expressed significantly more *BRh* photoreceptors than females (Chi-square: $p\text{-}value < 0.001$).

Based on the proteins detected in the R1 and R2 photoreceptors, we then inferred that there are at least six ommatidial types within the eye of *M. helenor* (Fig. 1 C-E), and we characterized the distribution of these ommatidial types in males and females. Chi-square testing shows a significant difference between male and female ommatidium distribution (Chi-square: $p\text{-}value < 0.001$). In males, the most abundant ommatidial type is *BRh-BRh*, representing approximately 35% of receptors compared to approximately 25% of ommatidia in females (Figure S3). Overall, our results thus show similar ommatidial types in males and females of *M. helenor*, and sexual dimorphism in the proportion of these different types of ommatidia.

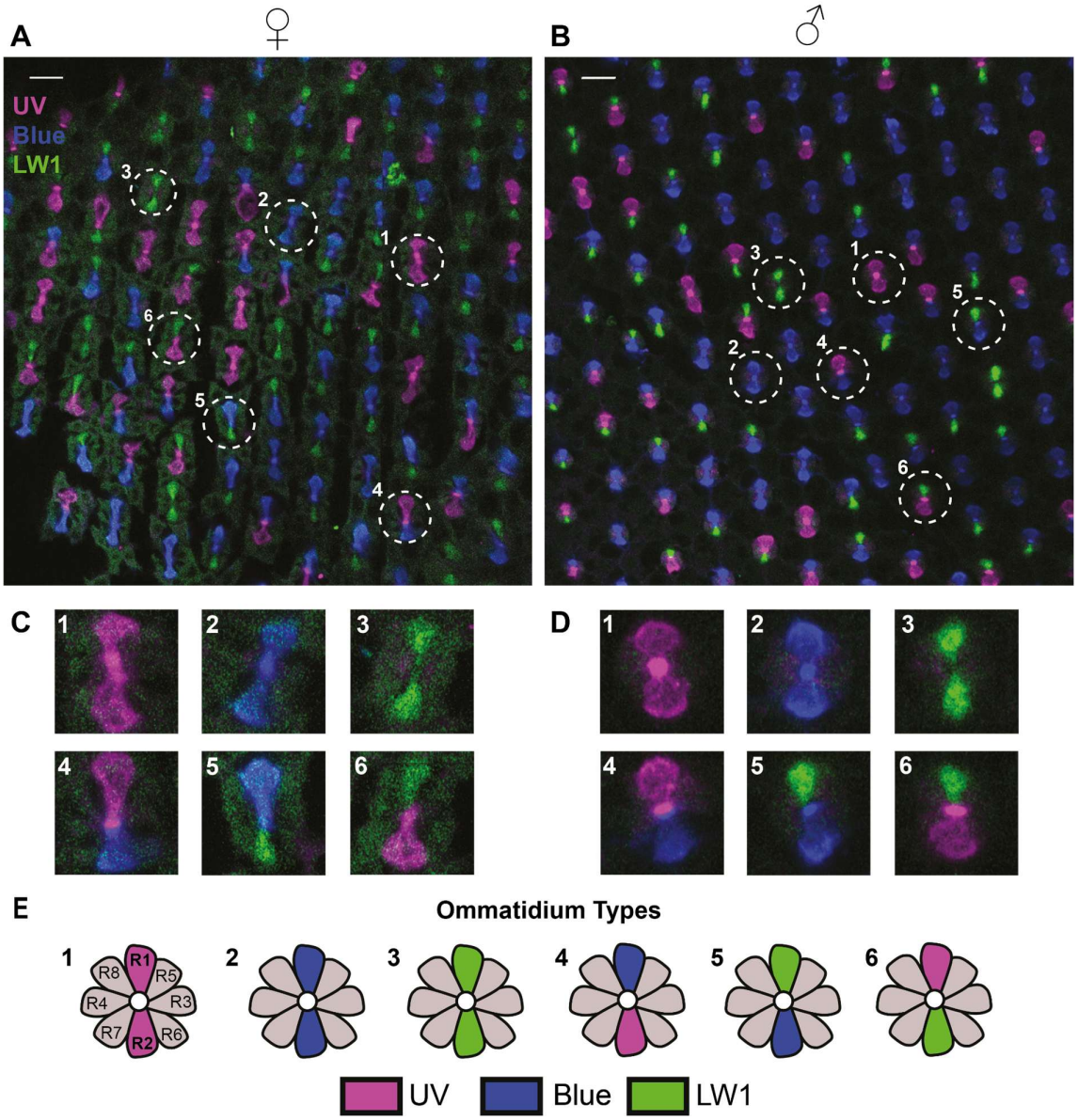

[Figure 1. Characterization of opsin protein expression in the different ommatidia of males and females *M. helenor*. Anti-BRh (blue), anti-LW1Rh (green), and anti-UVRh (magenta) antibody staining of (A) female and (B) male *M. helenor* retina. Scale bars represent 20 microns. Individual ommatidium types identified in (C) female and (D) male retina based on BRh, LW1Rh, and UVRh opsin expression. (J) Cartoon of the at least six ommatidia types based on opsin expression in the R1 and R2 photoreceptor cells of *M. helenor.*]

Opsin diversification at the genus scale in Morpho *butterflies.*

In order to study the evolution of opsin genes throughout the *Morpho* genus, we used *Morpho* genome assemblies from (Bastide et al. 2022) and (López Villavicencio et al. 2024) to retrieve the opsin sequences from additional *Morpho* species. The *UVRh*, *BRh* and *LWRh* genes detected in the genome of *M. helenor* were also found in the assembled genomes of 14 other *Morpho* species (*M. marcus*, *M. eugenia*, *M. granadensis*, *M. amathonte*, *M. menelaus*, *M. deidamia*, *M. achilles*, *M. godartii*, *M. telemachus*, *M. hecuba, M. theseus, M. niepelti, M. cypris* and *M. rhetenor).* All 15 species contain the complete coding sequences of the five opsins, covering all 8 exons. Because the *LWRh* gene was found in three distinctive copies in all 15 assembled species, the two duplication events are not limited to *M. helenor*, but rather likely occurred before the diversification of the *Morpho* genus. The analysis of the transcriptome of the eyes of *M. achilles, M. deidamia, M. hecuba, M. rhetenor and M. marcus* males showed that all five opsin genes are expressed in the eyes of those species (Table S2). These results suggest that the five *UVRh*, *BRh*, *LW1Rh*, *LW2Rh* and *LW3Rh* genes could be fully functional and involved in color vision in understory species (*M. achilles, M. deidamia*), canopy species (*M. hecuba, M. rhetenor*) and phylogenetically basal species (*M. marcus*).

Complementarily, we used PCR amplification to retrieve the opsin sequences of the *Morpho* species for which assembled genomes were not available. The PCR amplification allowed to retrieve some partial genomic *LW2Rh and LW3Rh* opsin sequences (6 exons) in 3 additional *Morpho* species (*M. aurora, M. sulkowskyi* and *M. cisseis*). We thus obtained opsin sequences for 18 *Morpho* species out of 30, including blue and non-blue species, inhabiting both the canopy and the understory (Figure 2).

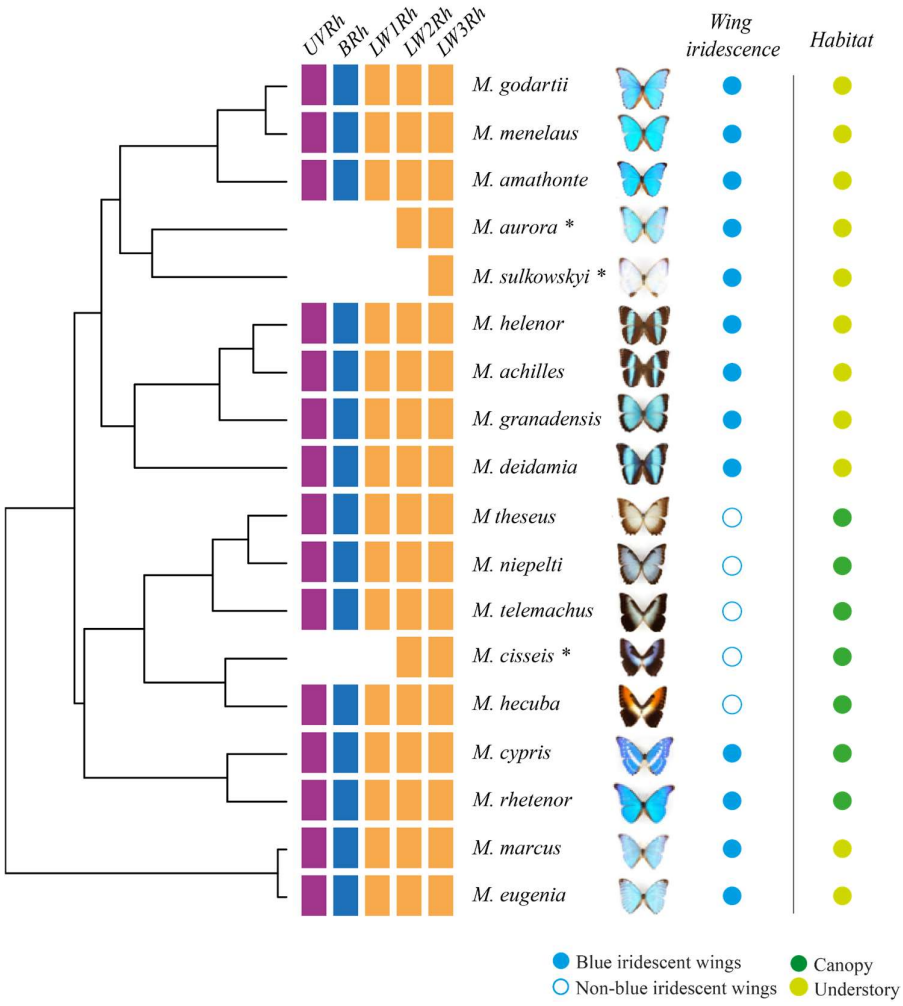

219

220 **[Figure 2: Opsin duplications and ecological and morphological characteristics of the 18 species**
221 **of the genus *Morpho* used in this study.** The phylogenetic relationships among the studied species was
222 retrieved from the phylogeny published in (Chazot et al. 2021)). The colored tiles show the retrieved
223 *UVRh*, *BRh*, *LW1Rh*, *LW2Rh* and *LW3Rh* opsin genes for each *Morpho* species. The opsin sequences
224 retrieved from the species marked with black stars were amplified using PCR and are thus only partial
225 sequences. Note that the absence of some opsins in species where whole-genome sequence was not
226 available is more likely due to a lack of amplification because of genetic divergence between species,
227 rather than an actual absence of the genes. The male dorsal wing pattern (Wing color: filled blue symbols
228 = blue-iridescent wings *vs.* open symbols = non blue-iridescent wings), and the habitat (Habitat: light-
229 green symbols = understory species *vs.* dark-green symbols = canopy species) is provided for each
230 studied species.]

The phylogenetic reconstruction of the partial *LWRh* genes of *Morpho* butterflies (Figure 3) showed that the *LW3Rh* gene is the most divergent gene compared to the other two *LW1Rh* and *LW2Rh* genes.

The phylogeny of the *LW3Rh* gene follows the phylogenetic species tree of the *Morpho* genus. However, the extensive length of the branch of the *LW3Rh* opsin of *M. eugenia* and *M. marcus* might stem from a particular selective regime acting on the visual sensitivities in these two species. The history of the *LW1Rh* and *LW2Rh* duplications reveals a slightly more complex pattern. For instance, the *LW1Rh* and *LW2Rh* genes of *M. eugenia* and *M. marcus* have a contrasted history as compared to the other species and do not branch with their respective *LW1Rh* and *LW2Rh* clade formed by the rest of the *Morpho* species. This pattern suggests that the 6 exons used to reconstruct this tree may undergo a different regime of selection in *M. marcus* and *M. eugenia* than on the other branches. Note that when reconstructing the phylogenetic tree of the *LWRh* opsins using only complete sequences (with less individuals but covering 8 exons), *LW1Rh* and *LW2Rh* genes from *M. marcus* and *M. eugenia* both branch at the base of their respective monophyletic clade (Figure S4), further suggesting that different regime of selection might only affect some specific exons.

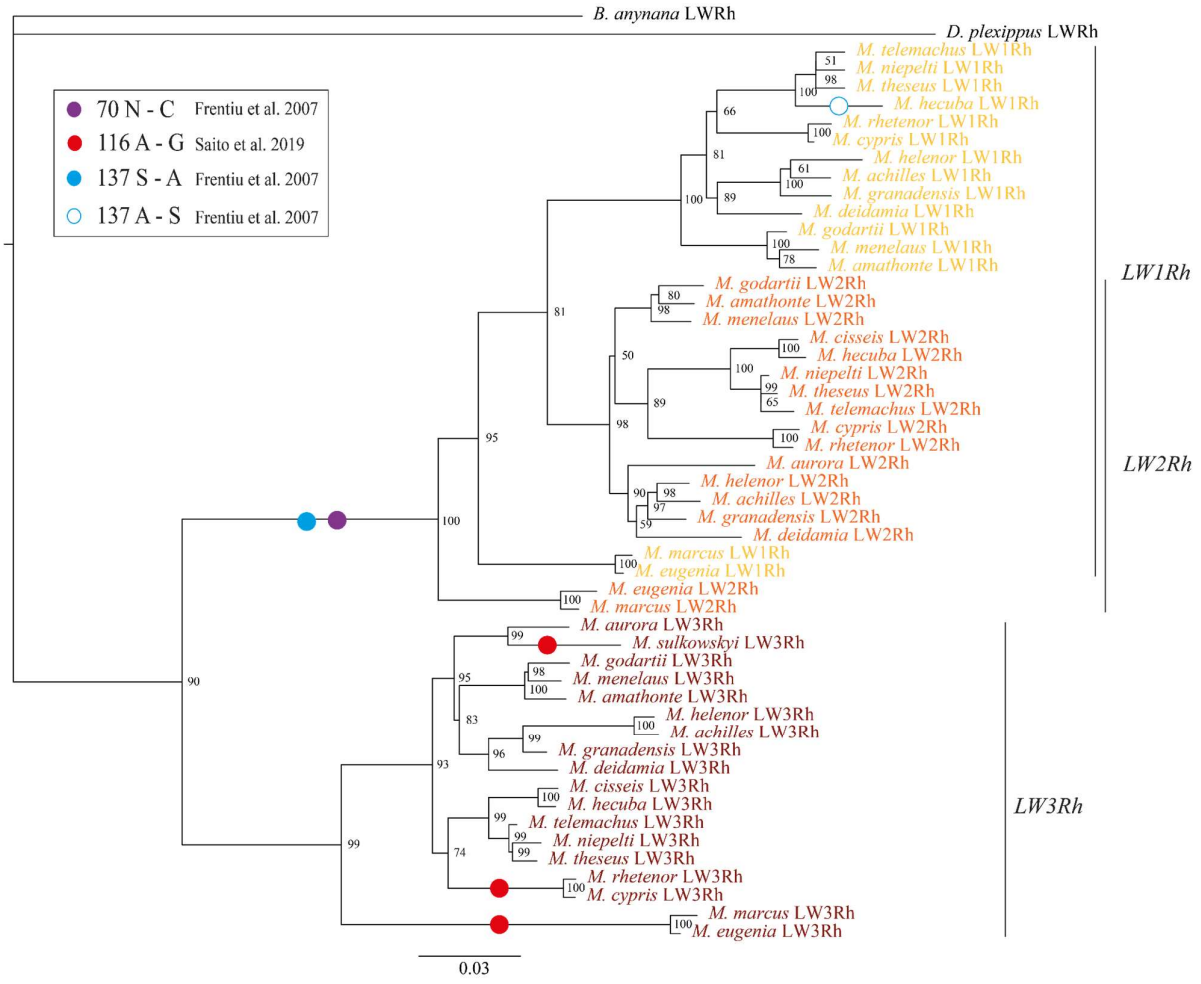

247

248 **[Figure 3: Maximum likelihood gene tree for the partial 6 exon sequences of *LWRh Morpho* opsins**
249 **and amino acid substitutions associated with putative spectral sensitivity shifts.** The gene tree was
250 inferred using IQtree under a TIM2e+I+G4 evolutionary model estimated with the ModelFinder option
251 using nucleotide *LWRh* sequences. Bootstrap values for each node are represented in the tree. The long
252 wavelength opsins of *Bicyclus anynana* (GenBank number: AY918895.2, (Frentiu et al. 2007)) and
253 *Danaus plexippus* (GenBank number: AY605545.1, (Sauman et al. 2005)) were used as outgroups.
254 *LW3Rh* genes are shown in dark-red, *LW2Rh* genes in orange and *LW1Rh* genes in yellow. We used
255 colored dots to designate amino acid substitutions found on the *LWRh* sequences of *Morpho* associated
256 with a spectral shift in other butterfly species (respective AA from (Frentiu et al. 2007) are numbered
257 on *Limenitis archippus archippus* and AA from (Saito et al. 2019) are numbered on bovine rhodopsin.
258 The homologous *Morpho* numbering can be found in Table S3).]

Variations at spectral tuning sites: evidence of putative spectral sensitivity shifts in BRh *and* LWRh *opsin genes in the* Morpho *genus.*

Because the amino acid sequence of a photoreceptive protein determines its capacity to absorb specific wavelengths, we checked whether variations of amino acids associated with tuning sites known in other butterflies could be observed in *Morpho* species. Amino acid numberings are taken from the original sources (Frentiu et al. 2007; Wakakuwa et al. 2010; Frentiu et al. 2015; Saito et al. 2019; Liénard et al. 2021) but the equivalent *Morpho* numbering is given in Table S3.

BRh opsin tuning sites

Compared to previous observations made on other butterflies, *Morpho BRh* opsin sequences are composed of amino acids associated with visual blue sensitivity shifts such as S116, F177 (Wakakuwa et al. 2010; Frentiu et al. 2015; Liénard et al. 2021) and R216 (Frentiu et al. 2015). A F177Y substitution is observed in two blue *Morpho* living in the canopy (*M. rhetenor* and *M. cypris*) and two blue *Morpho* living in the understory (*M. amathonte* and *M. godartii*) only, suggesting that the absorption of the *BRh* protein of those species might be slightly red-shifted compared to the other *Morpho* species. However, the amino acid sequences of *M. rhetenor* and *M. cypris* are also composed of A301 (Frentiu et al. 2015), an amino acid associated with subtle blue sensitivity shifts, suggesting that some amino acid shifts are unique to blue canopy species (see Figure S5 and Figure S6). Functional validation is still needed to understand the combined effect of substitutions associated with putatively opposite effects.

LWRh opsins tuning sites

The amino acid changes involved in spectral shifts detected among *Morpho LWRh* opsins are shown in Figure 3. The amino acid changes N70S and S137A are both correlated with a blue spectral shift of the L-opsin absorption in nymphalid butterflies (Frentiu et al. 2007). In *Morpho*, the S137A amino acid change occurred in the *LW1Rh* and *LW2Rh* lineages but not in the *LW3Rh* opsin, suggesting the *LW1Rh*

and *LW2Rh* opsin proteins might be sensitive to shorter wavelengths than the *LW3Rh* protein. Interestingly, a A137S reversion was found in the *LW1Rh* opsin of the non-blue canopy species *M. hecuba,* which could thus have a *LW1Rh* protein with a closer sensitivity to the *LW3Rh* protein compared to the other *Morpho* species.

Amongst the amino acid changes linked with a spectral shift of the protein, some can also cause red absorption shifts. For instance, the A116G amino acid change shifts the maximum of absorbance of opsins toward red wavelengths (Saito et al. 2019). In *Morpho*, the corresponding amino acid change occurs in the *LW3Rh* opsin protein for five species only, including 2 blue canopy species (*M. rhetenor* and *M. cypris*) and 3 blue understory species (*M. marcus*, *M. eugenia* and *M. sulkowskyi*, see Figure 3, Figure S7).

The blue-shifting amino acid mutations in the *LW1Rh* and *LW2Rh* protein sequences and red-shifting amino acid mutations in the *LW3Rh* opsin sequences strongly suggest that the duplicated *Morpho LWRh* opsins might be sensitive to different long wavelengths, consistent with the evolution of divergent visual systems in the *Morpho* genus.

Evidence of positive selection on the BRh *and* LW3Rh Morpho *opsin genes*

We then studied the ratio between non-synonymous and synonymous substitutions in the coding sequence of the different *Morpho* opsins ($dN/dS=\omega$) to characterize the selection regime acting on the evolution of the five opsin sequences. No signal of pervasive positive selection was found on the 5 *Morpho* opsin genes using random site models implemented in PAML (Table S4). However, we found significant evidence of episodic positive selection on the *BRh* opsin gene ($\omega_{BRh} = 4.890$, $p\text{-value} = 0.002$) and the *LW3Rh* opsin gene ($\omega_{BRh} = 2.89$, $p\text{-value} < 0.0001$) using BUSTED at a gene-wide scale (Table S5). A FUBAR analysis was run on those two genes to identify specific positively selected amino acid sites (Table S6). The sites 113, 189, 224, 232, 246, 310 and 363 (site numbering relative to *Morpho* opsins) were found to be under positive selection in the *BRh* opsin gene, and the sites 88, 133, 136, 179,

183, 205, 224, 229, 236, 305 and 318 showed signatures of positive selection in the *LW3Rh* gene. While none of these sites corresponds to known tuning sites in other butterfly species, they are either located near those sites or in the vicinity of the chromophore (see Figure 4).

To investigate the potential change in evolutionary rates among the three *LWRh* opsin duplications, we performed branch-site models to test for positive selection on different *LWRh* tree branches (see Methods). All branch-site models testing for positive selection on the *LWRh* tree came out non-significant. We also tested for positive selection in the branch leading to the *M. rhetenor*/*M. cypris* pair (the only two blue iridescent *Morpho* species living in the canopy) vs. the rest of the tree in the *BRh* gene and found no signal of positive selection on these branches (Table S7).

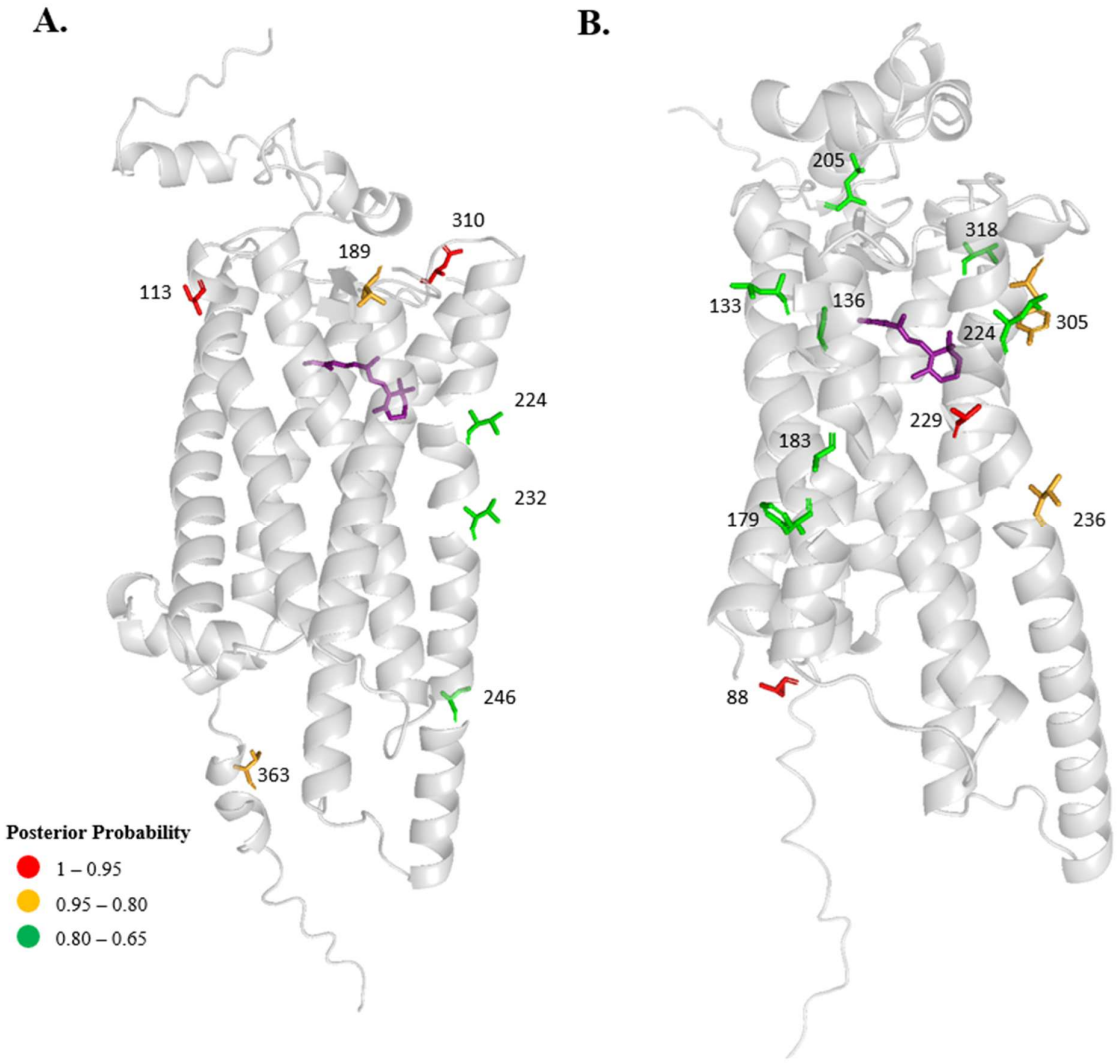

322

323 **[Figure 4: Positive selection on the *BRh* (A) and *LW3Rh* (B) opsin proteins in *Morpho*.** The amino
324 acids detected by the FUBAR analysis are represented in stick figures, and colored depending on their
325 probability of being under positive selection (posterior probabilities): from 65 to 80% (green), from 80
326 to 95% (orange) and from 95% to 100% (red). The approximated chromophore location is pictured in
327 purple.]

328

329

330

331

332 *Testing for ecological factors influencing the evolution of* Morpho *opsins.*

333 We looked for shifts in selective regimes acting on the sequences of the five *Morpho* opsin genes
334 depending on the species ecologies, using the CmC PAML model. We specifically annotated the *BRh*,
335 *UVRh*, and *LWRh* opsin trees depending on their wing phenotype and habitat (Figure 5, statistical
336 analyses in Table S8).

337

338 First, we found a significant effect of wing coloration on the evolution of the *LW2Rh* and *LW3Rh* genes,
339 with the species exhibiting blue wings having a higher ω than the non-blue species (*LW2Rh*:
340 $\omega_{LW3Rh\_Blue} = 0.61$ *vs.* $\omega_{LW3Rh\_Non\text{-}blue} = 0.00$ and *LW3Rh*: $\omega_{LW3Rh\_Blue} = 0.91$ *vs.* $\omega_{LW3Rh\_Non\text{-}blue} = 0.03$).
341 Second, the CmC analysis based on the habitat distribution of *Morpho* suggests that *UVRh* and *LW3Rh*
342 opsins show different evolutionary rates between understory and canopy species, with canopy species
343 having a higher ω*UVRh* than understory species ($\omega_{UVRh\_canopy} = 0.55$ *vs.* $\omega_{UVRh\_understory} = 0.31$), while the
344 trend is reversed for the *LW3Rh* gene ($\omega_{LW3Rh\_canopy} = 0.22$ *vs.* $\omega_{LW3Rh\_understory} = 0.77$). Finally, when
345 performing a clade model on the global phylogeny of the *LWRh* genes, comprising the data for *LW1Rh*,
346 *LW2Rh* and *LW3Rh*, both the wing color partition and the habitat partition were significant, with blue
347 species having a higher ω than the non-blue species ($\omega_{LWRh\_Blue} = 0.23$ *vs.* $\omega_{LWRh\_Non\text{-}blue} = 0.14$), and
348 understory species having a higher ω than the canopy species ($\omega_{LWRh\_canopy} = 0.09$ *vs.*
349 $\omega_{LWRh\_understory} = 0.24$).

350

351

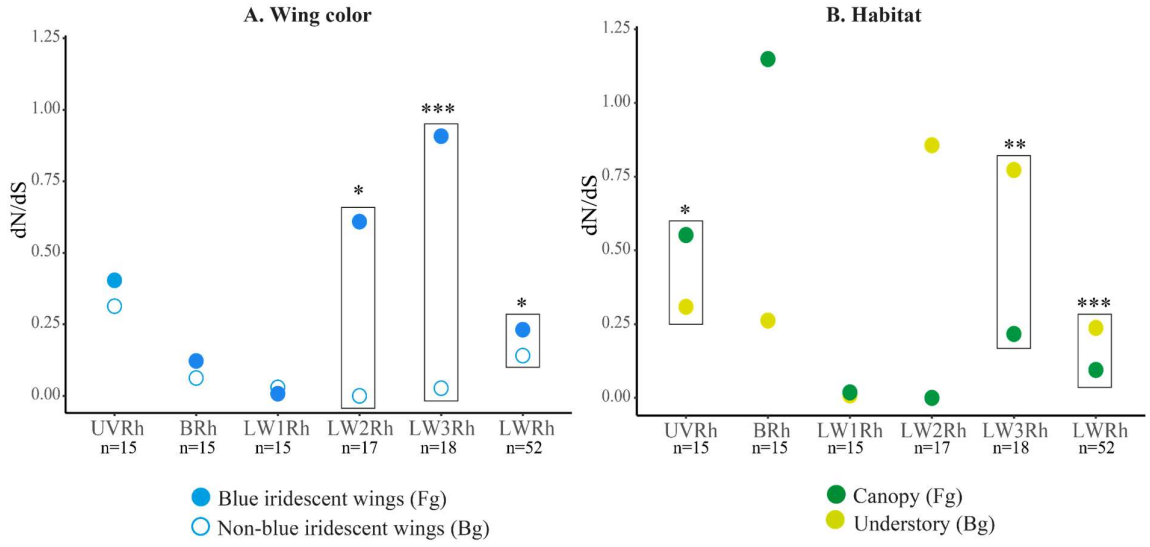

352

353 **[Figure 5: Variation of Morpho opsin *dN/dS* depending on wing coloration (A), habitat (B) and**
354 **Light environment (C).** The *dN/dS* of blue species are marked in blue, in white for non-blue species,
355 in dark-green in canopy species, in light-green in understory (Fg = foreground, Bg = background). The
356 number of analyzed genes are shown below each opsin type.]

357

358 *Evidence of correlated amino acid evolution between* LWRh *opsin genes.*

359 Finally, we used the Evo-Scope pipeline (Godfroid et al. 2024) to determine whether the evolution of
360 some amino acids in *Morpho* opsins could influence the evolution of other amino acids within the same
361 protein or impact the evolution of the sequence of other opsin proteins. The Evoscope analysis showed
362 signals of correlated evolution between amino acids both (1) within the same opsin protein and (2)
363 among different *LWRh* proteins (Figure 6, statistical analysis in Table S9).

364 Within the *LW3Rh* opsin protein, several amino acids exhibiting a significant signal of correlated
365 evolution were located in areas characterized by a high density of tuning sites and sites under positive
366 selection (between sites 131 and 145), suggesting a hot-spot of adaptive evolution in this region of the
367 protein. In particular, site 134, located near two sites under positive selection (133 and 136) and two
368 tuning sites (137 and 140), has been identified as being linked to the evolution of site 138. The Evoscope
369 results also highlighted that the evolution of the amino acids at site 134 can also induce the evolution of

amino acids at site 224, a site located near the chromophore of the protein, and showing signs of positive selection.

Interestingly, signals of correlated evolution were also found between amino acids belonging to different *LWRh* proteins: the evolution of two sites located in the *LW1Rh* protein and 3 sites in the *LW2Rh* protein was linked to the evolution of sites sitting in the *LW3Rh* protein. Among these sites of the *LW3Rh* proteins potentially influenced by the evolution of the other two *LWRh* opsins, two sites (site 135 and site 140) were located in the previously identified hotspot zone (between sites 131 and 145).

We separately analyzed the correlated evolution of the amino acids found within the *BRh* opsin protein (Figure S8) and the *UVRh* opsin protein (Figure S9) respectively. We found only two pairs of amino acids evolving under correlated evolution in the *UVRh* protein. In the *BRh* protein, some pairs of amino acids are located next to known tuning sites for this protein, but we found no hotspot zone similar to the one found in the *LW3Rh* protein.

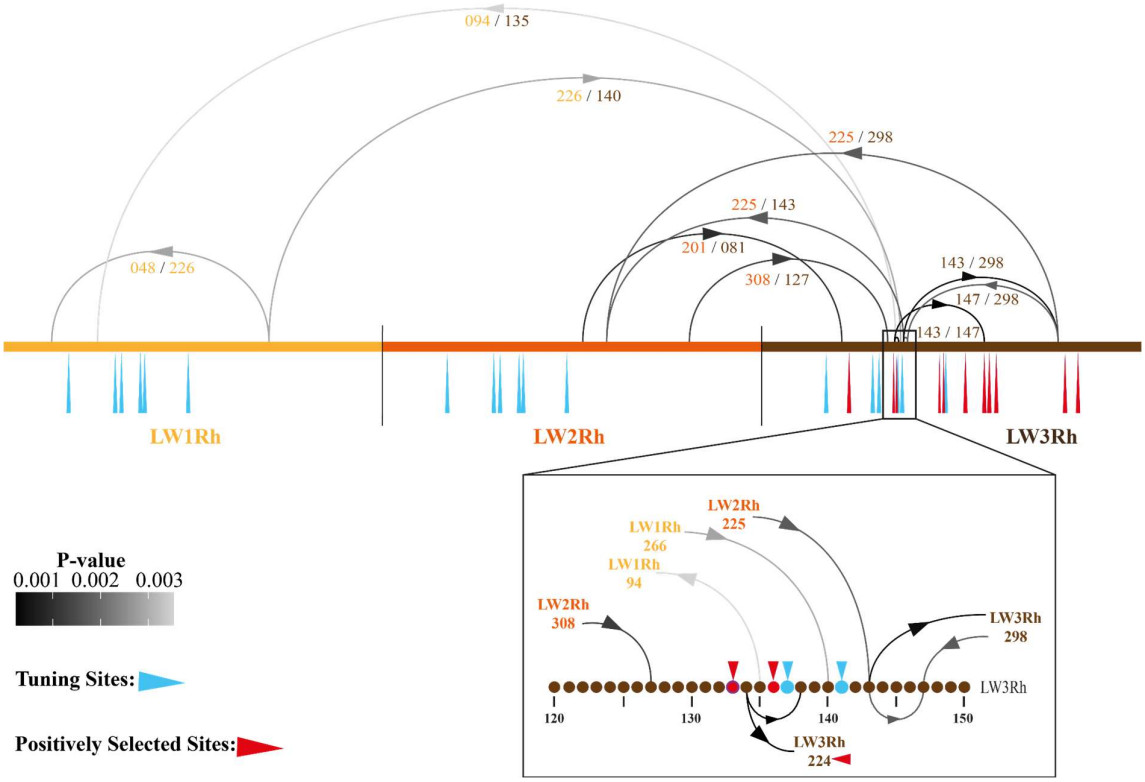

[Figure 6: Correlated amino-acid evolution within and between the three *LWRh* opsins observed throughout the genus *Morpho*. The sequence of the *LW1Rh* protein is colored in yellow, the sequence of the *LW2Rh* is colored in orange and the *LW3Rh* protein is colored in dark-red. The tuning sites and the positively selected sites are located on each protein using blue and red arrows respectively. The amino acid correlations detected by Evo-scope are represented by arcs coloured depending on the p-value for each test, using arrows to represent the direction of the induction and displaying the amino acid numbering involved in the correlated evolution. The hotspot zone identified in the *LW3Rh* protein is highlighted in the box.]

Discussion

Duplications and patterns of expression of opsins form a peculiar visual system in M. helenor.

The RNA expression analyses performed on *M. helenor* eye tissue confirmed that all 5 opsin genes, including the three different *LWRh* copies, are expressed in the eyes of *M. helenor* butterflies from both sexes. Our immunohistochemical assays then showed that *UVRh* and *BRh* opsins are expressed in R1 and R2 photoreceptive cells, consistent with previous observations in other butterfly visual systems (*e.g. Vanessa cardui*, (Briscoe et al. 2003); *Heliconius*, (McCulloch et al. 2017); *Danaus plexippus*, (Sauman et al. 2005); *Pieris rapae*, (Arikawa et al. 2005)). Surprisingly, *LW1Rh* expression in *M. helenor* was restricted to the R1-R2 receptive cells, and we did not detect any co-expression of *BRh*, *UVRh* or *LW1Rh* in any cell type. This *LWRh* pattern of expression is uncommon among various butterfly families as long-wavelength sensitive opsin genes are usually expressed in R3 to R8 cells (Briscoe 2008). However, these results are consistent with previous polarization sensitivity measurements performed on the eyes of *M. helenor* (Pirih et al. 2022), showing that R1 and R2 cells are strongly sensitive to UV and Blue light, and also sensitive to Green or Green/Yellow light, which could be absorbed by *LW1Rh* opsins. Although we were not able to characterize the pattern of expression of the *LW2Rh* and *LW3Rh* proteins in the eyes of *Morpho*, we assume these are likely to be expressed in cells R3 to R8 because these cells are also sensitive the Green and Yellow light according to the polarisation sensitivity reported in (Pirih et al. 2022). We thus described 6 different ommatidial types in *M. helenor* (Figure 1), but unknown *LW2Rh* or *LW3Rh* expression patterns may increase the number of possible ommatidia types in *M. helenor*.

This peculiar expression pattern of opsins is also associated with a sexually dimorphic expression pattern of some opsins in *M. helenor*. In particular, higher RNA *LW1Rh* expression was found in the eyes of females, supported by a higher *LW1Rh* photoreceptor count at the protein level. Furthermore, a high number of *BRh* photoreceptors was found in males *M. helenor* eyes, associated with a high frequency of *BRh-BRh* ommatidia types in males compared to females (see Figure S3). Such sexual dimorphism

in opsin protein expression has been reported in several taxa, and can take many forms: sexual dimorphism can encompass variation in opsin co-expression in different eye photoreceptor cells (Sison-Mangus et al. 2006), the lack of opsin expression in a photoreceptor cell of one sex compared to the other (McCulloch et al. 2017), and variations in the number of photoreceptor cells (Hilbrant et al. 2014). Sexual dimorphism could arise from different selective pressures affecting the evolution of the visual systems of males and females. For instance, the behaviors of *Morpho* males and females strongly differ: in the wild, males display a typical patrolling behavior and show a striking response to blue stimuli (Le Roy et al. 2021). On the other hand, females tend to fly in dense forest areas and to spend time locating and flying around host-plants. Those different ecological conditions encountered by males and females might generate divergent selection on visual systems. Long-distance detection of blue color might be advantageous in males searching for females and might promote increased sensitivity to blue wavelengths. Although *M. helenor* males do not have duplicated *BRh* opsin genes as other blue sensitive butterflies (Lycaenids, (Sison-Mangus et al. 2006); Pieridae, (Arikawa et al. 2005; Awata et al. 2009; Wakakuwa et al. 2010)), their retina is composed of a higher proportion of *BRh-BRh* photoreceptors than other blue butterflies (Sison-Mangus et al. 2006). In contrast, discrimination in the green wavelength might be promoted in females, because of the significance of host-plant detection in this sex, as suggested in other butterflies with sexually-dimorphic visual sensitivities (Finkbeiner and Briscoe 2021).

The novelty of the *M. helenor* eye organization compared to other butterflies and the number of expressed opsin genes in its visual system shows a divergent evolution of opsin gene expression in *Morpho* butterflies as compared to other Nymphalidae, that may result in the evolution of color discrimination capacities.

Light environment and wing iridescence strongly influence the evolution of the genes involved in the visual system of Morpho.

449 The five opsin genes described in *M. helenor* were also found in the genome of 14 additional *Morpho*
450 species. RNA expression data confirmed that those five genes are expressed in the eyes of all tested
451 species, suggesting that this specific visual system organization might likely be ancestral to the
452 diversification of *Morpho*. While neutral evolution contributes to the divergence of opsin genes among
453 species, the divergent selection generated by the different biotic and abiotic conditions encountered in
454 the different micro-habitats occupied by the different species could also impact the evolution of the
455 opsin sequences across the genus.

456

457 Models testing for episodic positive selection on the 5 opsin genes revealed significant signals of
458 positive selection mostly on the sequences of *BRh* and *LW3Rh* genes. Since several positively selected
459 sites detected in our study are located close to previously-documented tuning sites and/or close to the
460 chromophore, our results are consistent with an effect of selection on the diversification of visual
461 sensitivities in those genes.

462 First, the analysis of the amino acid sequence of the *BRh* gene in *Morpho* showed that four species
463 exhibit amino acid changes involving known tuning sites. In particular, *M. rhetenor* and *M. cypris*, the
464 only two blue *Morpho* species living in the canopy in this dataset, display amino acid substitutions at
465 two different tuning sites, that could putatively cause shifts in visual perception. This result suggests
466 that *M. rhetenor* and *M. cypris* could have a different visual perception than the rest of the *Morpho*
467 genus. However, no significant signal of selection specific to this lineage was found, suggesting that this
468 difference might be due to phylogenetic divergence only. Overall, we found that the evolutionary rate
469 of the *BRh* opsin was not significantly different between canopy and understory species, and surprisingly
470 did not find a correlation between the evolution of the *BRh* opsin sequences and the presence or absence
471 of blue iridescent coloration on the wings of *Morpho* butterflies. In the context of mate choice or male-
472 male competition, we would expect that blue visual perception would be different between blue and
473 non-blue species. Interestingly, while spectral sensitivity data suggest that the blue absorbing cells of
474 *M. helenor* might be sensitive to approximately 450 nm (Pirih et al. 2022), iridescence quantification

475 showed that the peak of reflectance of *M. helenor* wings can vary from 350 nm to 500 nm (UV/purple
476 to green) depending on the angle of illumination (Ledamoisel et al. 2025), suggesting that different color
477 signals generated by the wings might be processed by other opsin genes during mate searching.

478 In line with this hypothesis, we found that *LWRh* genes are very diversified among *Morpho*. Our results
479 show that some amino acid substitutions found on those proteins could be associated with different
480 spectral shifts affecting the three *LWRh* gene copies: indeed, *LW1Rh* and *LW2Rh* tend to bear blue-
481 shifting amino acids as compared to *LW3Rh*. Although functional validation is needed, the *LW3Rh*
482 protein could thus be responsible for the absorption peak found in *Morpho* at 570 nm in (Pirih et al.
483 2022), while the *LW1Rh* and *LW2Rh* proteins could be associated with the absorbance peaks found at
484 505nm and 551nm (Pirih et al. 2022). Long-wavelength sensitive opsin diversification has been reported
485 in a number of taxa (fishes: (Watson et al. 2011); Hemiptera: (Xu et al. 2021); Coleoptera: (Sharkey et
486 al. 2021); Anurans: (Schott et al. 2022)) including butterflies (*Papilio xuthus*, (Briscoe 2008)), and is
487 often associated with change in light habitats and/or niche differentiation (Carleton et al. 2020). In
488 *Morpho*, we found that the *dN/dS* of the *LW2Rh* and *LW3Rh* opsins of the blue iridescent species is
489 significantly higher than the *dN/dS* of the *LW2Rh* and *LW3Rh* genes of the non-blue iridescent species,
490 consistent with higher rate of adaptive evolution of *LWRh* genes in blue iridescent species. Such
491 evolution might have been promoted by selection favouring detection and discrimination of the blue-
492 green iridescent signals displayed by the wings of blue *Morpho* species. Interestingly, we also found
493 that the evolutionary rate of the *LW3Rh* gene is significantly higher in the *Morpho* species living in the
494 understory compared to those living in the canopy. The understory habitat is dominated by vegetation:
495 as the discrimination of subtle long-wavelength color variation might be advantageous in a forest
496 environment in terms of foraging and oviposition (Kelber 1999), this habitat is likely an important driver
497 of green/red color discrimination in *Morpho*. The understory is also a darker environment than the
498 canopy: in particular, the amount of UV-light is significantly reduced in the understory in tropical forests
499 compared to the canopy (Brown et al. 1994; Nilsson et al. 2022). The higher evolutionary rate of the
500 *UVRh* opsin in the canopy as compared to understory species suggests that heterogeneous light
501 availability might have influenced the evolution of this specific opsin gene in those habitats.

The co-occurrence of mutations between sites located on different opsin proteins suggests a joint evolution of LWRh *genes.*

Because wavelength discrimination by the visual systems depends on the shape of sensitivity peaks and on the distance among them, controlled by the respective sensitivities of each opsin protein, its evolution might involve integrated changes across the different opsin genes. To assess this coevolution, we specifically tested for correlated shifts in amino acids both within and among opsins.

Within the *LW3Rh* protein, five pairs of amino acid sites displayed a significant signal of correlated evolution, meaning that a change of amino acid at site A was found to coincide with a change of amino acid at site B more often than expected by chance given the *Morpho* phylogeny. Because purifying selection tends to promote mutations that would stabilize the structure or the function of a protein, coupled amino acid evolution within a protein is expected: amino acid substitutions at a site could compensate for deleterious substitutions at other sites of the protein (Pál et al. 2006). However, amino acid changes could also be driven by adaptation. Considering the direct link between amino acid sequence and wavelength sensitivity (Hofmann and Lamb 2023), this seems particularly plausible in opsin proteins. Amino acid variations in the *LW3Rh* revealed correlated evolution between 2 pairs of sites located very close (1 or 2 sites away) to either known tuning sites in butterflies, or positively selected sites detected by our previous analysis. Among those, site 134 was found to induce amino acid changes at the positively selected site 224, highlighting the intertwined evolution of key-sites in specific areas of the protein.

Moreover, we also found co-occurring mutations between amino acid sites belonging to different *LWRh* proteins, suggesting concerted evolution among those three genes. Specifically, we show that mutations found on specific amino acid sites in *LW1Rh* co-evolved with mutations found on LW3Rh amino acid sites close to tuning sites, in what looks like a hotspot of adaptive evolution. Correlated mutations between proteins have been extensively observed between proteins part of a network and physically

528 interacting with one another (Pazos et al. 1997), but correlations in the evolution of genes sharing
529 functional relationships are much less documented. Yet, visual perception can be seen as the result of
530 the integration of visual signals absorbed by different opsin proteins, potentially creating an indirect link
531 between the evolution of those genes, whether in the form of shared regulatory mechanisms or similar
532 evolutionary forces. For example, following an opsin duplication, the gain of function of the new protein
533 could impact the selection regime of the other to maintain fine-tuned spectral sensitivity. It is the case
534 in Lycaenidae where coordinated shifts of amino acids have been found in the *BRh* and *LWRh* opsins,
535 enhancing their visual perception (Liénard et al. 2021). Although our approach is only correlative and
536 functional validation is needed, it underlines the importance of studying the molecular co-evolution of
537 opsins, because of the extensive evolutionary tinkering involved in the diversification of visual system

538

539 Conclusions

540 Altogether, our results evidence the peculiar evolution of visual systems in closely-related species
541 evolving in divergent microhabitats and illustrate how the evolution of the different opsins protein
542 properties and patterns of expression may be shaped by the specific selective pressures generated by
543 different micro-habitats or contrasted sexual selection. By jointly studying the correlated evolution of
544 different genes as well as their spatial pattern of expression, our study highlights the multiple pathways
545 enabling the evolution of visual discrimination capacities finely-tuned by selective processes.

546

547 Materials and Methods

548 Characterisation of opsins expression and spatial localisation in *Morpho helenor*

549 *Testing RNA differential expression between males and females* M. helenor

550 We used the previously assembled genome of *M. helenor* (Bastide et al. 2022) to retrieve the sequence
551 of the 5 opsin genes (*BRh*, *UVRh*, *LW1Rh*, *LW2Rh* and *LW3Rh*) found in this *Morpho* species. In order

552 to test whether opsin genes were expressed in *Morpho helenor* tissues, the eye transcriptome of five
553 males and five females *M. helenor theodorus* were sequenced. The specimens were purchased from a
554 breeding farm located in Ecuador (Quinta De Goulaine, https://quintadegoulaine.com/es/papillons.php)
555 and raised in insectaries at STRI in Gamboa, Panama, between January and March 2023. The Qiagen
556 RNAeasy Mini Kit was used to extract the RNA of each sample following the manufacturer's
557 instructions. Library preparation and Illumina sequencing were performed at the Ecole normale
558 supérieure GenomiqueENS core facility (Paris, France). Messenger (polyA+) RNAs were purified from
559 250 ng of total RNA using oligo(dT). Libraries were performed using the strand specific RNA-Seq
560 library preparation *Stranded mRNA Prep, Ligation kit* (Illumina) and were multiplexed by 39 on a P3
561 flowcell (Illumina). A 118 bp single end read sequencing was performed on a NextSeq 2000 device
562 (Illumina). The analyses were performed using the Eoulsan pipeline (Jourdren et al. 2012), including
563 read filtering, mapping, and alignment filtering. Before mapping, poly N read tails were trimmed, reads
564 ≤40 bases were removed, and reads with quality mean ≤30 were discarded. Reads were then aligned
565 against the *Morpho helenor* genome using STAR version 2.7.8a (Dobin et al. 2013). Alignments from
566 reads matching more than once on the reference genome were removed using Java version of samtools
567 (Li et al. 2009). To compute gene expression, the *Morpho helenor* genome annotation was used. All
568 overlapping regions between alignments and referenced exons were counted and aggregated by genes
569 using FeatureCounts v2.0.6 (Liao et al. 2014). The sample counts were normalized using DESeq2 1.42.1
570 (Love et al. 2014). Statistical treatments and differential analyses were also performed using DESeq2
571 1.42.1, using an adjusted p-value threshold set at 0.05.

572 The number of opsin reads was extracted and their relative expression was analyzed separately from the
573 rest of the transcriptome, and Kruskall-Wallis tests were used to test for the effect of sex in the number
574 of expressed opsin reads. To account for the multiple testing on the 5 opsin genes, we use a Bonferroni
575 test to compute adjusted p-values.

576

577 *Spatial distribution of opsin protein within* Morpho helenor *eyes revealed by immunohistochemistry*

We used an immunohistochemistry approach to locate the opsin proteins within the eyes of *M. helenor*. First, we used the translated amino acid sequences of *M. helenor UVRh, BRh*, *LW1Rh*, *LW2Rh,* and *LW3Rh* opsins to identify antigenic, accessible, and unique peptides as candidate targets for polyclonal antibody production. An antibody against the peptide GIVKQVFAHEAALRE in the loop domain between helix 5 and 6 of *UVRh* was generated in guinea pigs, an antibody against the peptide GWNIPEEHQDLVHE in the N-terminus domain of *BRh* was generated in goat, an antibody against a peptide GSDTGPGISC in the N-terminus domain of *LW1Rh* was generated in rabbit (Biosynth International, Gardner, MA, USA).

Then, we purchased *M. helenor* pupae from Costa Rica Entomological Supply to test these specific antibodies on fresh eyes. Upon delivery, pupae were hung in greenhouse enclosures where they were housed post-eclosure and until processing. Butterflies freely flew in the enclosures and fed on moistened orange slices. Five male and five females were processed for immunohistochemistry.

Methods were adapted from previous studies (Hsiao et al. 2012; Perry et al. 2016; McCulloch et al. 2017; Chakraborty et al. 2023). Butterflies were euthanized by quickly crushing the thorax and beheading them. In 1x PBS, the heads were bisected and excess tissue was removed under a dissecting scope. The eyes were fixed in 4% paraformaldehyde for 30 minutes in a cold room (approximately 15 °C) with rotation. Fixed eyes then underwent step-wise sucrose baths (10, 20, then 30% sucrose in 1x PBS) for two hours for each step in a 15°C cold room with rotation. The corneal lenses of the eyes were carefully removed under a dissecting scope, and each eye was then embedded in gelatin-albumin blocks. Blocks were then fixed in 4% formalin (in 1x PBS) for 15 hours at 4 °C. Embedded tissue gelatin-albumin blocks were sliced with a Precisionary Compresstome VF-310-0Z to 60 micron slices. Slices were blocked in a blocking solution of 5% (v/v) normal donkey serum and 0.3% triton-X in 1x PBS (0.3% PBST) for one hour at room temperature. The slices were incubated overnight at 4 °C with primary antibodies (1:200 goat anti-Blue, 1:100 guinea pig anti-UVRh, and 1:100 rabbit anti-LW1 in blocking solution). Afterwards, the slides underwent five washes with 0.3% PBST for 15 minutes per wash at room temperature. The slides were then incubated overnight in darkness at 4 °C with secondary antibodies (1:250 donkey anti-goat AlexaFluor 488, 1:250 donkey anti-guinea pig AlexaFluor 647, and

1:250 donkey anti-rabbit Cy3 in blocking solution). Again, they were washed five times with 0.3% PBST for 15 minutes per wash and mounted in 70% glycerol. Images were taken using a Zeiss LSM 900 Airyscan 2 confocal microscope under a 20x/0.8NA dry objective in the UC Irvine Optical Core Facility and exported using ZenBlue 3.5.

Investigating the evolution of opsin sequences throughout the Morpho genus

Retrieving the opsin sequences from 15 Morpho *reference genomes*

The visual opsin sequences of 8 *Morpho* species observed in the understory habitat (*M. helenor*, *M. marcus*, *M. eugenia*, *M. granadensis*, *M. amathonte*, *M. menelaus*, *M. deidamia*, *M. achilles)* and 3 *Morpho* species found in the canopy habitat (*M. telemachus*, *M. hecuba,* and *M. rhetenor)* were retrieved from the annotations of the *Morpho* genome assemblies published in (Bastide et al. 2022) and (López Villavicencio et al. 2024). Four additional genomes including 1 understory species (*M. godartii*) and 3 canopy species (*M. theseus*, *M. niepelti* and *M. cypris*) were specifically obtained for this study and their sequencing, assembly and annotation were performed following the same pipeline as described in (López Villavicencio et al. 2024). Among the 30 *Morpho* species described in the literature (Chazot et al. 2021), we thus had access to the genomic data of 15 *Morpho* species scattered across the phylogeny. Overall, one *UVRh*, one *BRh* and three *LWRh* (referred to as *LW1Rh*, *LW2Rh* and *LW3Rh* hereafter) opsin genes were identified within each of these 15 genomes. To compare opsin gene positions across all *Morpho* species with available chromosome level assemblies, we scaffolded *Morpho* contigs against the *Maniola jurtina* chromosome-level assembly (ilManJurt1.1) using RagTag (Alonge et al. 2022). All scaffolds were renamed to match the chromosome nomenclature of *M. jurtina*.

Sequencing of eye transcriptome of six Morpho *species*

To check for opsin RNA expression in different *Morpho* species scattered across the phylogeny of the genus, the eyes of freshly caught males belonging to 5 sympatric species from French Guiana (*M.*

630 *achilles*, *M. deidamia*, *M. hecuba*, *M. rhetenor* and *M. marcus*), were dissected and stored in RNAlater
631 at -80°C before extraction. RNA was extracted using the Qiagen RNeasy Mini Kit according to the
632 manufacturer's instructions and stored at −80 °C until use. The transcriptome of each sample was
633 sequenced using Nanopore technology. Library preparation and Nanopore sequencing were performed
634 at the Ecole normale supérieure GenomiqueENS core facility (Paris, France). 10 ng of total RNA were
635 amplified and converted to cDNA using a modified version of the protocol described in (Guilcher et al.
636 2021). Briefly, the ligation and rRNA depletion steps were skipped and the oligo
637 GCAGGGGAAATCATCAGCGTATAACTTTTTTTTTTTTTTTTTTTTTTTTTTTVN was used
638 for the first strand cDNA synthesis. The oligos
639 TTTCTGTTGGTGCTGATATTGCAAGCAGTGGTATCAACGCAGAGTAC and
640 ACTTGCCTGTCGCTCTATCTTCGCAGGGGAAATCATCAGCGTATAAC were used for the
641 amplification of the full-length cDNAs. Afterwards an average of 15 fmol of amplified cDNA was used
642 for the library preparation. After the PCR adapter ligation, a 0,6X Agencourt Ampure XP beads clean-
643 up was optimised and 2 fmol of the purified product was taken into PCR for amplification and barcodes
644 addition with a 17 minutes elongation at each 18 cycles (barcodes from SQK-PCB111, ONT). Samples
645 were pooled in equimolar quantities to obtain 25 fmol of cDNA and the rapid adapter ligation step was
646 performed. Libraries were multiplexed by 9 on one flowcell FLO-PRO002 according to the
647 manufacturer's protocol. Sequencing was performed with the SQK-PCB111 72-hour sequencing
648 protocol run on the PromethION P2 solo, using the MinKNOW software (versions 5.9.12). A mean of
649 11 ± 2,8 million passing ONT quality filter reads was obtained for each of the samples. Base-calling
650 from read event data was performed by dorado-0.7.1 sup. Structural annotation was performed following
651 a custom protocol published in protocols.io (DOI:
652 dx.doi.org/10.17504/protocols.io.36wgqd5qyvk5/v1). The extracted reads were assembled on the
653 respective *Morpho* reference genomes from (Bastide et al. 2022) and (López Villavicencio et al. 2024)
654 and the RNA counts were extracted using FeatureCounts v2.0.6 (Liao et al. 2014). As we collected data
655 for only one individual per species, this analysis was used to assess the presence of expressed opsin
656 genes in the eyes of *Morpho* but not their absence, using TPM counts.

657

658 *Amplification of additional opsin sequences throughout the* Morpho *genus*

659 In order to retrieve the opsin sequences of the 15 *Morpho* species for which assembled genomes are not
660 available, the coding sequences of the *UVRh*, *BRh* and *LWRh* opsins from *M. helenor* and *M. telemachus*
661 were used to design specific PCR primers (see Table S10) targeting these three genes with Primer3
662 (Untergasser et al. 2012).

663 PCRs were performed on these 15 *Morpho* species, using DNA samples from collection specimens
664 stored in the National Museum of Natural History in Paris, France. The DNA of those *Morpho* was
665 extracted using the Qiagen extraction DNeasy Blood Tissue Kits. Each PCR reaction was run using
666 20µL of solution containing 11.25µL of water, 4µL of Buffer 5X for Taq LongAmp, 1.25µL of dNTPs
667 (6.6mM), 1µL of BSA (5mg/mL), 0.625µL of DMSO, 0.475µL of primers (10pM), 0.375µL of Taq
668 LongAmp (ThermiFischer) and 3µL DNA. The thermal cycling conditions for the amplification started
669 with a 30s denaturation at 94°C, followed by a gradual decrease of the hybridization temperature during
670 18 PCR cycles, from 61°C to 52°C, and a 10 min elongation step at 65°C (touch-down method). For the
671 following 50 cycles, the hybridization temperature was fixed to 52°C.

672 The PCR products were sequenced using the short-read Illumina technology. The Geneious Prime
673 program (2022.1.1 version) was then used to reconstruct the whole opsin sequences. Adding to the 15
674 *Morpho* species already studied from *Morpho* genomes, this method allowed to retrieve partial *LWRh*
675 opsin sequences for 2 other understory species (*M. aurora*, *M. sulkowskyi*) and 1 canopy species (*M.*
676 *cisseis*).

677

678 *Sequence alignment and tree reconstruction*

679 The coding opsin sequences (exons only) of each opsin, retrieved from 18 *Morpho* species, were aligned
680 using the MUSCLE algorithm (Edgar 2004) implemented in MEGA X (Tamura et al. 2021). As our
681 *UVRh* and *BRh* opsin sequence dataset is composed of complete sequences only, the phylogenetic tree

682 of the *UVRh* and *BRh* opsins were generated using the alignment of those complete genes (8 exons)
683 across 15 *Morpho* species. However, because the *LW1Rh*, *LW2Rh* and *LW3Rh* opsins sequence dataset
684 contains both complete (*i.e.* whole-genome based) and partial opsin (*i.e.* PCR based) sequences, we
685 generated the associated *LWRh* phylogenetic tree using an alignment of the 6 exons sequences in all
686 species studied (n = 18). Independent phylogenetic trees were also generated for the *LW1Rh*, *LW2Rh*
687 and *LW3Rh* genes respectively, allowing for separate analyses within each *LWRh* copy. IQtree (Nguyen
688 et al. 2015) was used to generate the phylogenies, and the ModelFinder option (Kalyaanamoorthy et al.
689 2017) was used to select the best respective evolutionary models for each tree. Nodes' robustness was
690 estimated using Ultrafast Bootstrap (Hoang et al. 2018) on 10000 iterations.

691

692 *Detection of amino-acids changes acting on spectral sensitivity*

693 To identify amino acid changes associated with changes in spectral sensitivity in other butterfly species,
694 we used data from the literature (Frentiu et al. 2007; Wakakuwa et al. 2010; Frentiu et al. 2015; Saito et
695 al. 2019; Liénard et al. 2021) to locate so-called tuning sites within the *BRh* and *LWRh* opsin sequences
696 of the *Morpho* butterflies studied here. We used the MUSCLE algorithm (Edgar 2004) implemented in
697 MEGA X (Tamura et al. 2021) to align the *Morpho* opsin sequences to the opsin sequences of other
698 butterfly species to find the tuning-sites in *Morpho*. This method allows identifying whether the amino
699 acids variations observed among *Morpho* species detected in our positive selection analyses are likely
700 to modify the sensitivity to different wavelengths.

701

702 *Detection of signature of selection acting on the evolution of opsin sequences*

703 To characterize the selection regime acting on the evolution of opsin sequences and assess departure
704 from neutral evolution, we studied the ratio between the non-synonymous (*dN*) and synonymous (*dS*)
705 mutations in the coding sequences of the different opsins $\omega=dN/dS$. A gene with a higher non-
706 synonymous substitution rate compared to its synonymous substitution rate ($\omega>1$) is said to be under
707 positive selection. The *codeml* program from the software package PAML 4.9j (Yang and others 1997)

was used to test for gene-wide pervasive selection acting on the evolution of visual opsins. To investigate whether selection is acting on specific codons in every branch of the opsin gene trees, we performed model comparisons using several optional models proposed by PAML (Site Models M0, M1a, M2a, M7, M8). First, to ensure the selective pressure varies among the codons of opsin genes, the M0 model was compared to the M1a model. Then, the M2a and M8 models were used to assess positive selection on each opsin gene, by comparing their prediction to their respective null models M1a and M7. A Bayes Empirical Bayes (BEB) analysis was used to identify the positively selected amino acids among the genes under positive selection. As PAML's Site Model is not suited to detect gene-wide selection occurring only in a few subsets of branches and sites, we also used the BUSTED program (Murrell et al. 2015) from the software HYPHY v2.5.65 (Kosakovsky Pond et al. 2020) to test for episodic selection on *Morpho* opsin genes. This method uses a mixed effects model allowing ω to vary across sites and branches, and detects signature of selection happening on at least one branch. For genes showing significant results, we applied the FUBAR program (Murrell et al. 2013) to identify specific amino acids evolving under positive selection across lineages. The gene trees used for PAML's site model, BUSTED and FUBAR are available in Figure S10.

Additionally, PAML's branch-site models were also computed to estimate the selective pressures acting at specific codon sites within different lineages of the *LWRh* gene phylogeny. In order to test whether the duplicated *LWRh* opsin genes follow distinct regimes of selection, the branches of the gene phylogeny were partitioned into three clades comprising the branches leading to (1) the *LW1Rh* genes, (2) the *LW2Rh* genes and (3) the *LW3Rh* genes, excluding *M. marcus* and *M. eugenia* branches. We generated three distinct branch-site models to test whether the ω of those clades were different from the ω of the branches of the rest of the phylogeny. As *M. eugenia* and *M. marcus*, the most basal species of the phylogeny, seem to follow a peculiar evolution, the branches leading to (1) the *LW1Rh* genes, (2) the *LW2Rh* genes and (3) the *LW3Rh* genes of those two species were also used as "foreground" branches and to generate three additional branch-site models (see Figure S11 for branch annotations). Furthermore, we also used PAML's branch site model to test for positive selection in specific branches

of the *BRh* gene, especially to look for any specific pattern of selection in the pair *M. rhetenor*/*M. cypris* vs. the rest of the phylogeny. To assess positive selection, the results of the branch-site models were compared to their respective null models, which assume the same ω among all branches.

Finally, in order to test the effects of ecological factors on the evolution of opsin sequences, while accounting for phylogenetic relationships between species, we used a clade model (PAML's Cmc Model: M2a_rell (null) vs. Model C) to analyze putative differential evolution of the opsin genes between species sharing a blue iridescent phenotype and others (Blue vs. Non-Blue), species living in the canopy or the understory (Canopy vs. Understory).

Detection of correlated amino acid evolution

We used the Evo-Scope pipeline described in (Godfroid et al. 2024) to determine whether the evolution of some amino acids in a given opsin protein could (i) influence the evolution of other amino acids within the same protein or (ii) impact the evolution of the sequence of other opsin proteins. The Evo-Scope pipeline was designed to study correlated evolution of biological discrete traits by accounting for the phylogenetic structure of the data. After a step of ancestral character reconstruction, a first tool (*epics*, (Behdenna et al. 2016) is used to identify pairs of co-occuring mutations on each branch of the tree. Second, after selecting the pairs of traits showing a significant signal of correlated evolution, the *epocs* method (Behdenna et al. 2022) determines which trait influences the evolution of the other under different scenarios among each pair.

In order to apply this method to our data, we considered each amino acid of the 3 partial *LWRh* opsin proteins (6 exons) as discrete traits to analyze the co-occurence of amino acid shifts found across the phylogeny. We applied this method only for the species for which we had the opsin data for the 3 LWRh genes (n = 15). As the gene trees of the 3 *LWRh* opsins are similar but not identical, we first performed Shimodaira-Hasegawa tests implemented in IQ-tree (Nguyen et al. 2015) to evaluate whether the likelihood difference between each gene's own topology and alternative trees was statistically different

(Table S11). As the *LW3Rh* gene tree showed the highest compatibility with the *LW1Rh*, *LW2Rh* and *LW3Rh* alignments, we used this phylogeny to study the correlated evolution of the amino acids found in the *LW1Rh*, *LW2Rh* and *LW3Rh* opsin genes. After identifying amino acid pairs showing signals of correlated evolution, we compared whether some of those amino acid sites were associated with known tuning sites or positively selected sites, to understand the global impact selection can have on the evolution of *LWRh* opsin proteins.

As *BRh* and *UVRh* genes are more divergent compared to the *LWRh* genes, we did not measure the correlated evolution of the amino acids of those three proteins. However, we computed the correlated evolution of the amino acids among BRh and UVRh opsins respectively.

Structural representation of opsin proteins

To locate the positively selected amino acid sites and the sites associated with a signal of correlated evolution within the protein and specifically their proximity to the chromophore, we predicted the 3D structure of the different opsins of *M. helenor* using the online platform CollabFold v 1.5.2 (Mirdita et al. 2022). The platform combines the Alphafold2 algorithm (Jumper et al. 2021) for protein structure prediction, and the model MMseq2 to generate the sequence alignments. The protein structures were edited in PyMOL (The PyMOL Molecular Graphic System, Version 2.6 Schrödinger, LLC) to highlight the amino acids previously detected as under positive selection. The putative chromophore location was inferred from the chromophore location determined in the jumping spider rhodopsin (Varma et al. 2019). Complementarily, we used Protter (Omasits et al. 2014) to generate a 2D representation of each gene and annotated it with the relevant amino acid sites detected in this study.

Data availability:

All sequences used for the analyses will be available on GenBank upon publication.

Acknowledgements:

The authors would like to thank Guillaume Achaz for the advice provided on the use of the EvoScope pipeline. We are also grateful to Owen McMillan from the Smithsonian Tropical Research Institute (Panama) for providing facilities to raise *M. helenor theodorus*. We thank Etienne Delannoy from the POPS facility (IPS2) for conducting with GenomiqueENS the adaptation of the ONT RNA-seq protocol. All the bioinformatic analyses were performed on the Plateforme de Calcul Intensif et Algorithmique PCIA (Muséum national d'histoire naturelle, Centre national de la recherche scientifique), the MeSU platform at Sorbonne-Université and the Genotoul bioinformatics platform Toulouse Occitanie (Bioinfo Genotoul, https://doi.org/10.15454/1.5572369328961167E12). We exported the eyes of *M. helenor theodorus* from Panama using exportation permit number PA-01-ARB-028-2023, and declared to the French authorities the exportation of butterfly eyes from French Guiana to the French metropole. J.L PhD was funded by an IBEES grant from Sorbonne Université. The GenomiqueENS core facility was supported by the France Génomique national infrastructure, funded as part of the "Investissements d'Avenir" program managed by the Agence Nationale de la Recherche (contract ANR-10-INBS-0009). This study was funded by the European Union (ERC-2022-COG - OUTOFTHEBLUE - 101088089) and by the Human Frontier Science Program grant (RGP005/2023, https://doi.org/10.52044/HFSP.RGP0052023.pc.gr.168591). Views and opinions expressed are however those of the authors only and do not necessarily reflect those of the European Union or the European Research Council. Neither the European Union nor the granting authority can be held responsible for them.

References

Alonge M, Lebeigle L, Kirsche M, Jenike K, Ou S, Aganezov S, Wang X, Lippman ZB, Schatz MC, Soyk S. 2022. Automated assembly scaffolding using RagTag elevates a new tomato system for high-throughput genome editing. *Genome Biol* 23:258.

Arikawa K. 2003. Spectral organization of the eye of a butterfly, Papilio. *J Comp Physiol A* 189:791–800.

Arikawa K, Wakakuwa M, Qiu X, Kurasawa M, Stavenga DG. 2005. Sexual Dimorphism of Short-Wavelength Photoreceptors in the Small White Butterfly, Pieris rapae crucivora. *J. Neurosci.* 25:5935–5942.

Awata H, Wakakuwa M, Arikawa K. 2009. Evolution of color vision in pierid butterflies: blue opsin duplication, ommatidial heterogeneity and eye regionalization in Colias erate. *J Comp Physiol A* 195:401–408.

Bastide H, López-Villavicencio M, Ogereau D, Lledo J, Dutrillaux A-M, Debat V, Llaurens V. 2022. Genome assembly of 3 Amazonian *Morpho* butterfly species reveals Z-chromosome rearrangements between closely related species living in sympatry. *GigaScience* 12:giad033.

Behdenna A, Godfroid M, Petot P, Pothier J, Lambert A, Achaz G. 2022. A Minimal yet Flexible Likelihood Framework to Assess Correlated Evolution. *Systematic Biology* 71:823–838.

Behdenna A, Pothier J, Abby SS, Lambert A, Achaz G. 2016. Testing for Independence between Evolutionary Processes. *Systematic Biology* 65:812–823.

Belušič G, Ilić M, Meglič A, Pirih P. 2021. Red-green opponency in the long visual fibre photoreceptors of brushfoot butterflies (Nymphalidae). *Proceedings of the Royal Society B: Biological Sciences* 288:20211560.

Brandon CS, Greenwold MJ, Dudycha JL. 2017. Ancient and Recent Duplications Support Functional Diversity of Daphnia Opsins. *J Mol Evol* 84:12–28.

Briscoe AD. 2008. Reconstructing the ancestral butterfly eye: focus on the opsins. *Journal of Experimental Biology* 211:1805–1813.

Briscoe AD, Bernard GD, Szeto AS, Nagy LM, White RH. 2003. Not all butterfly eyes are created equal: Rhodopsin absorption spectra, molecular identification, and localization of ultraviolet-, blue-, and green-sensitive rhodopsin-encoding mRNAs in the retina of Vanessa cardui. *Journal of Comparative Neurology* 458:334–349.

Briscoe AD, Bybee SM, Bernard GD, Yuan F, Sison-Mangus MP, Reed RD, Warren AD, Llorente-Bousquets J, Chiao C-C. 2010. Positive selection of a duplicated UV-sensitive visual pigment coincides with wing pigment evolution in Heliconius butterflies. *Proceedings of the National Academy of Sciences* 107:3628–3633.

Brown MJ, Parker GG, Posner NE. 1994. A Survey of Ultraviolet-B Radiation in Forests. *Journal of Ecology* 82:843–854.

Carleton KL, Escobar-Camacho D, Stieb SM, Cortesi F, Marshall NJ. 2020. Seeing the rainbow: mechanisms underlying spectral sensitivity in teleost fishes. *Journal of Experimental Biology* 223:jeb193334.

Chakraborty M, Lara AG, Dang A, McCulloch KJ, Rainbow D, Carter D, Ngo LT, Solares E, Said I, Corbett-Detig RB, et al. 2023. Sex-linked gene traffic underlies the acquisition of sexually dimorphic UV color vision in Heliconius butterflies. *Proceedings of the National Academy of Sciences* 120:e2301411120.

Chazot N, Blandin P, Debat V, Elias M, Condamine FL. 2021. Punctuational ecological changes rather than global factors drive species diversification and the evolution of wing phenotypes in Morpho butterflies. *J of Evolutionary Biology* 34:1592–1607.

Chazot N, Panara S, Zilbermann N, Blandin P, Le Poul Y, Cornette R, Elias M, Debat V. 2016. Morpho morphometrics: shared ancestry and selection drive the evolution of wing size and shape in Morpho butterflies. *Evolution* 70:181–194.

Chen P-J, Awata H, Matsushita A, Yang E-C, Arikawa K. 2016. Extreme Spectral Richness in the Eye of the Common Bluebottle Butterfly, Graphium sarpedon. *Front. Ecol. Evol.* [Internet] 4. Available from: https://www.frontiersin.org/journals/ecology-and-evolution/articles/10.3389/fevo.2016.00018/full

Detto T. 2007. The fiddler crab Uca mjoebergi uses colour vision in mate choice. *Proceedings of the Royal Society B: Biological Sciences* 274:2785–2790.

Dobin A, Davis CA, Schlesinger F, Drenkow J, Zaleski C, Jha S, Batut P, Chaisson M, Gingeras TR. 2013. STAR: ultrafast universal RNA-seq aligner. *Bioinformatics* 29:15–21.

Dollion AY, Herrel A, Marquis O, Leroux-Coyau M, Meylan S. 2020. The colour of success: does female mate choice rely on male colour change in the chameleon Furcifer pardalis? *Journal of Experimental Biology* 223:jeb224550.

Edgar RC. 2004. MUSCLE: multiple sequence alignment with high accuracy and high throughput. *Nucleic Acids Research* 32:1792–1797.

Finkbeiner SD, Briscoe AD. 2021. True UV color vision in a female butterfly with two UV opsins. *Journal of Experimental Biology* 224:jeb242802.

Franzke M, Kraus C, Dreyer D, Pfeiffer K, Beetz MJ, Stöckl AL, Foster JJ, Warrant EJ, el Jundi B. 2020. Spatial orientation based on multiple visual cues in non-migratory monarch butterflies. *Journal of Experimental Biology* 223:jeb223800.

Frentiu FD, Bernard GD, Sison-Mangus MP, Van Zandt Brower A, Briscoe AD. 2007. Gene Duplication Is an Evolutionary Mechanism for Expanding Spectral Diversity in the Long-Wavelength Photopigments of Butterflies. *Molecular Biology and Evolution* 24:2016–2028.

Frentiu FD, Yuan F, Savage WK, Bernard GD, Mullen SP, Briscoe AD. 2015. Opsin Clines in Butterflies Suggest Novel Roles for Insect Photopigments. *Molecular Biology and Evolution* 32:368–379.

Godfroid M, Coluzzi C, Lambert A, Glaser P, Rocha EPC, Achaz G. 2024. Evo-Scope: Fully automated assessment of correlated evolution on phylogenetic trees. *Methods in Ecology and Evolution* 15:282–289.

Godin JG, Dugatkin LA. 1996. Female mating preference for bold males in the guppy, Poecilia reticulata. *Proceedings of the National Academy of Sciences* 93:10262–10267.

Gomez D, Richardson C, Lengagne T, Derex M, Plenet S, Joly P, Léna J-P, Théry M. 2010. Support for a role of colour vision in mate choice in the nocturnal European treefrog (Hyla arborea). *Behaviour* 147:1753–1768.

Gröning J, Hochkirch A. 2008. Reproductive Interference Between Animal Species. *The Quarterly Review of Biology* 83:257–282.

Guilcher M, Liehrmann A, Seyman C, Blein T, Rigaill G, Castandet B, Delannoy E. 2021. Full Length Transcriptome Highlights the Coordination of Plastid Transcript Processing. *International Journal of Molecular Sciences* 22:11297.

Hilbrant M, Almudi I, Leite DJ, Kuncheria L, Posnien N, Nunes MD, McGregor AP. 2014. Sexual dimorphism and natural variation within and among species in the Drosophilaretinal mosaic. *BMC Evol Biol* 14:240.

Hoang DT, Chernomor O, Von Haeseler A, Minh BQ, Vinh LS. 2018. UFBoot2: improving the ultrafast bootstrap approximation. *Molecular biology and evolution* 35:518–522.

Hofmann KP, Lamb TD. 2023. Rhodopsin, light-sensor of vision. *Progress in Retinal and Eye Research* 93:101116.

Horth L. 2007. Sensory genes and mate choice: Evidence that duplications, mutations, and adaptive evolution alter variation in mating cue genes and their receptors. *Genomics* 90:159–175.

Hsiao H-Y, Johnston RJ, Jukam D, Vasiliauskas D, Desplan C, Rister J. 2012. Dissection and Immunohistochemistry of Larval, Pupal and Adult Drosophila Retinas. *J Vis Exp*:4347.

Jourdren L, Bernard M, Dillies M-A, Le Crom S. 2012. Eoulsan: a cloud computing-based framework facilitating high throughput sequencing analyses. *Bioinformatics* 28:1542–1543.

Jumper J, Evans R, Pritzel A, Green T, Figurnov M, Ronneberger O, Tunyasuvunakool K, Bates R, Žídek A, Potapenko A, et al. 2021. Highly accurate protein structure prediction with AlphaFold. *Nature* 596:583–589.

Kalyaanamoorthy S, Minh BQ, Wong TK, Von Haeseler A, Jermiin LS. 2017. ModelFinder: fast model selection for accurate phylogenetic estimates. *Nature methods* 14:587–589.

Kelber A. 1999. Ovipositing butterflies use a red receptor to see green. *Journal of Experimental Biology* 202:2619–2630.

Kosakovsky Pond SL, Poon AFY, Velazquez R, Weaver S, Hepler NL, Murrell B, Shank SD, Magalis BR, Bouvier D, Nekrutenko A, et al. 2020. HyPhy 2.5—A Customizable Platform for Evolutionary Hypothesis Testing Using Phylogenies. *Molecular Biology and Evolution* 37:295–299.

Le Roy C, Roux C, Authier E, Parrinello H, Bastide H, Debat V, Llaurens V. 2021. Convergent morphology and divergent phenology promote the coexistence of Morpho butterfly species. *Nature communications* 12:7248.

Ledamoisel J, Buatois B, Mauxion R, Andraud C, McClure M, Debat V, Llaurens V. 2025. Sending mixed signals: convergent iridescence and divergent chemical signals in sympatric sister-species of Amazonian butterflies. *eLife* [Internet] 14. Available from: https://elifesciences.org/reviewed-preprints/106098

Li H, Handsaker B, Wysoker A, Fennell T, Ruan J, Homer N, Marth G, Abecasis G, Durbin R, 1000 Genome Project Data Processing Subgroup. 2009. The Sequence Alignment/Map format and SAMtools. *Bioinformatics* 25:2078–2079.

Liao Y, Smyth GK, Shi W. 2014. featureCounts: an efficient general purpose program for assigning sequence reads to genomic features. *Bioinformatics* 30:923–930.

Liénard MA, Bernard GD, Allen A, Lassance J-M, Song S, Childers RR, Yu N, Ye D, Stephenson A, Valencia-Montoya WA, et al. 2021. The evolution of red color vision is linked to coordinated rhodopsin tuning in lycaenid butterflies. *Proceedings of the National Academy of Sciences* 118:e2008986118.

López Villavicencio M, Ledamoisel J, Poloni R, Lopez-Roques C, Debat V, Llaurens V. 2024. Increased Evolutionary Rate in the Z chromosome of Sympatric and Allopatric Species of Morpho Butterflies. *Genome Biology and Evolution* 16:evae227.

Love MI, Huber W, Anders S. 2014. Moderated estimation of fold change and dispersion for RNA-seq data with DESeq2. *Genome Biology* 15:550.

Luehrmann M, Cortesi F, Cheney KL, de Busserolles F, Marshall NJ. 2020. Microhabitat partitioning correlates with opsin gene expression in coral reef cardinalfishes (Apogonidae). *Functional Ecology* 34:1041–1052.

Maan ME, van der Spoel M, Jimenez PQ, van Alphen JJM, Seehausen O. 2006. Fitness correlates of male coloration in a Lake Victoria cichlid fish. *Behavioral Ecology* 17:691–699.

McCulloch KJ, Macias-Muñoz A, Mortazavi A, Briscoe AD. 2022. Multiple Mechanisms of Photoreceptor Spectral Tuning in Heliconius Butterflies. *Molecular Biology and Evolution* 39:msac067.

McCulloch KJ, Yuan F, Zhen Y, Aardema ML, Smith G, Llorente-Bousquets J, Andolfatto P, Briscoe AD. 2017. Sexual Dimorphism and Retinal Mosaic Diversification following the Evolution of a Violet Receptor in Butterflies. *Molecular Biology and Evolution* 34:2271–2284.

Mirdita M, Schütze K, Moriwaki Y, Heo L, Ovchinnikov S, Steinegger M. 2022. ColabFold: making protein folding accessible to all. *Nat Methods* 19:679–682.

Murphy MJ, Westerman EL. 2022. Evolutionary history limits species' ability to match colour sensitivity to available habitat light. *Proceedings of the Royal Society B: Biological Sciences* 289:20220612.

Murrell B, Moola S, Mabona A, Weighill T, Sheward D, Kosakovsky Pond SL, Scheffler K. 2013. FUBAR: A Fast, Unconstrained Bayesian AppRoximation for Inferring Selection. *Molecular Biology and Evolution* 30:1196–1205.

Murrell B, Weaver S, Smith MD, Wertheim JO, Murrell S, Aylward A, Eren K, Pollner T, Martin DP, Smith DM, et al. 2015. Gene-Wide Identification of Episodic Selection. *Molecular Biology and Evolution* 32:1365–1371.

Musilova Z, Salzburger W, Cortesi F. 2021. The Visual Opsin Gene Repertoires of Teleost Fishes: Evolution, Ecology, and Function. *Annu. Rev. Cell Dev. Biol.* 37:441–468.

Nguyen L-T, Schmidt HA, Von Haeseler A, Minh BQ. 2015. IQ-TREE: a fast and effective stochastic algorithm for estimating maximum-likelihood phylogenies. *Molecular biology and evolution* 32:268–274.

Nilsson D-E, Smolka J, Bok M. 2022. The vertical light-gradient and its potential impact on animal distribution and behavior. *Front. Ecol. Evol.* [Internet] 10. Available from: https://www.frontiersin.org/journals/ecology-and-evolution/articles/10.3389/fevo.2022.951328/full

Omasits U, Ahrens CH, Müller S, Wollscheid B. 2014. Protter: interactive protein feature visualization and integration with experimental proteomic data. *Bioinformatics* 30:884–886.

Pál C, Papp B, Lercher MJ. 2006. An integrated view of protein evolution. *Nat Rev Genet* 7:337–348.

Pazos F, Helmer-Citterich M, Ausiello G, Valencia A. 1997. Correlated mutations contain information about protein-protein interaction 1. *Journal of Molecular Biology* 271:511–523.

Pérez i de Lanuza G, Carazo P, Font E. 2014. Colours of quality: structural (but not pigment) coloration informs about male quality in a polychromatic lizard. *Animal Behaviour* 90:73–81.

Perry M, Kinoshita M, Saldi G, Huo L, Arikawa K, Desplan C. 2016. Molecular logic behind the three-way stochastic choices that expand butterfly colour vision. *Nature* 535:280–284.

Pirih P, Ilić M, Meglič A, Belušič G. 2022. Opponent processing in the retinal mosaic of nymphalid butterflies. *Philosophical Transactions of the Royal Society B: Biological Sciences* 377:20210275.

Ricci V, Ronco F, Boileau N, Salzburger W. 2023. Visual opsin gene expression evolution in the adaptive radiation of cichlid fishes of Lake Tanganyika. *Science Advances* 9:eadg6568.

Saito T, Koyanagi M, Sugihara T, Nagata T, Arikawa K, Terakita A. 2019. Spectral tuning mediated by helix III in butterfly long wavelength-sensitive visual opsins revealed by heterologous action spectroscopy. *Zoological Lett* 5:35.

Sandkam B, Young CM, Breden F. 2015. Beauty in the eyes of the beholders: colour vision is tuned to mate preference in the Trinidadian guppy (Poecilia reticulata). *Molecular Ecology* 24:596–609.

Sauman I, Briscoe AD, Zhu H, Shi D, Froy O, Stalleicken J, Yuan Q, Casselman A, Reppert SM. 2005. Connecting the Navigational Clock to Sun Compass Input in Monarch Butterfly Brain. *Neuron* 46:457–467.

Schott RK, Fujita MK, Streicher JW, Gower DJ, Thomas KN, Loew ER, Bamba Kaya AG, Bittencourt-Silva GB, Guillherme Becker C, Cisneros-Heredia D, et al. 2024. Diversity and Evolution of Frog Visual Opsins: Spectral Tuning and Adaptation to Distinct Light Environments. *Molecular Biology and Evolution* 41:msae049.

Schott RK, Perez L, Kwiatkowski MA, Imhoff V, Gumm JM. 2022. Evolutionary analyses of visual opsin genes in frogs and toads: Diversity, duplication, and positive selection. *Ecology and Evolution* 12:e8595.

Sharkey CR, Powell GS, Bybee SM. 2021. Opsin Evolution in Flower-Visiting Beetles. *Front. Ecol. Evol.* [Internet] 9. Available from: https://www.frontiersin.org/journals/ecology-and-evolution/articles/10.3389/fevo.2021.676369/full

Sison-Mangus MP, Bernard GD, Lampel J, Briscoe AD. 2006. Beauty in the eye of the beholder: the two blue opsins of lycaenid butterflies and the opsin gene-driven evolution of sexually dimorphic eyes. *Journal of Experimental Biology* 209:3079–3090.

Sison-Mangus MP, Briscoe AD, Zaccardi G, Knüttel H, Kelber A. 2008. The lycaenid butterfly Polyommatus icarus uses a duplicated blue opsin to see green. *Journal of Experimental Biology* 211:361–369.

Smith EJ, Partridge JC, Parsons KN, White EM, Cuthill IC, Bennett ATD, Church SC. 2002. Ultraviolet vision and mate choice in the guppy (Poecilia reticulata). *Behavioral Ecology* 13:11–19.

Smith WC, Goldsmith TH. 1990. Phyletic aspects of the distribution of 3-hydroxyretinal in the class insecta. *J Mol Evol* 30:72–84.

1013 Sondhi Y, Ellis EA, Bybee SM, Theobald JC, Kawahara AY. 2021. Light environment drives
1014 evolution of color vision genes in butterflies and moths. *Commun Biol* 4:1–11.

1015 Stavenga DG, Arikawa K. 2006. Evolution of color and vision of butterflies. *Arthropod Structure &*
1016 *Development* 35:307–318.

1017 Tamura K, Stecher G, Kumar S. 2021. MEGA11: Molecular Evolutionary Genetics Analysis Version
1018 11. *Molecular Biology and Evolution* 38:3022–3027.

1019 Untergasser A, Cutcutache I, Koressaar T, Ye J, Faircloth BC, Remm M, Rozen SG. 2012. Primer3—
1020 new capabilities and interfaces. *Nucleic Acids Research* 40:e115.

1021 Varma N, Mutt E, Mühle J, Panneels V, Terakita A, Deupi X, Nogly P, Schertler GFX, Lesca E. 2019.
1022 Crystal structure of jumping spider rhodopsin-1 as a light sensitive GPCR. *Proc. Natl. Acad.*
1023 *Sci. U.S.A.* 116:14547–14556.

1024 Wakakuwa M, Stavenga DG, Kurasawa M, Arikawa K. 2004. A unique visual pigment expressed in
1025 green, red and deep-red receptors in the eye of the small white butterfly, Pieris rapae
1026 crucivora. *Journal of Experimental Biology* 207:2803–2810.

1027 Wakakuwa M, Terakita A, Koyanagi M, Stavenga DG, Shichida Y, Arikawa K. 2010. Evolution and
1028 Mechanism of Spectral Tuning of Blue-Absorbing Visual Pigments in Butterflies.Warrant EJ,
1029 editor. *PLoS ONE* 5:e15015.

1030 Watson CT, Gray SM, Hoffmann M, Lubieniecki KP, Joy JB, Sandkam BA, Weigel D, Loew E,
1031 Dreyer C, Davidson WS, et al. 2011. Gene Duplication and Divergence of Long Wavelength-
1032 Sensitive Opsin Genes in the Guppy, Poecilia reticulata. *J Mol Evol* 72:240–252.

1033 Xu P, Lu B, Chao J, Holdbrook R, Liang G, Lu Y. 2021. The evolution of opsin genes in five species
1034 of mirid bugs: duplication of long-wavelength opsins and loss of blue-sensitive opsins. *BMC*
1035 *Ecol Evo* 21:66.

1036 Yang Z, others. 1997. PAML: a program package for phylogenetic analysis by maximum likelihood.
1037 *Computer applications in the biosciences* 13:555–556.

1038 Zaccardi G, Kelber A, Sison-Mangus MP, Briscoe AD. 2006. Color discrimination in the red range
1039 with only one long-wavelength sensitive opsin. *Journal of Experimental Biology* 209:1944–
1040 1955.

1041 Zhang S. 2012. Visually Guided Decision Making in Foraging Honeybees. *Front. Neurosci.* [Internet]
1042 6. Available from:
1043 https://www.frontiersin.org/journals/neuroscience/articles/10.3389/fnins.2012.00088/full

1044

1045

1046

1047